RANDOM MATRIX SPECTRA AND RELAXATION IN COMPLEX NETWORKS*

Reimer Kühn

Mathematics Department, King's College London
Strand, London WC2R 2LS, UK

(Received January 12, 2015)

We evaluate spectra of stochastic matrices defined on complex random graphs, with edges (i, j) of a graph being given positive random weights $W_{ij} > 0$ in such a fashion that column sums are normalized to one. The structure of the graphs and the distribution of the non-zero edge weights W_{ij} are largely arbitrary. We only require that the mean vertex degree remains finite in the thermodynamic limit, and that the W_{ij} satisfy a detailed balance condition. The main motivation for this work derives from the fact that knowing the spectra of stochastic matrices is tantamount to knowing the complete spectrum of relaxation times of stochastic processes described by them. One of the interesting new phenomena uncovered by our study is the appearance of localization transitions and mobility edges in the spectra of stochastic matrices of the type investigated in the present study.

DOI:10.5506/APhysPolB.46.1653
PACS numbers: 02.50.–r, 05.10.–a

1. Introduction

The principal aim of the present contribution is to describe ways in which the spectral theory of sparse random matrices can be harnessed to study random walks and relaxation phenomena in complex networks.

The study of complex networks and random graphs has gained considerable momentum in the last 15 years [1–5]. This has, in no small part, been driven by the rapid spread of network-based information and communication technologies, as well as pervasive trends towards increasing levels of socio-economic and financial interdependencies, which are transforming societies across the globe.

* Presented at the Conference "Random Matrix Theory: Foundations and Applications", Kraków, Poland, July 1–6, 2014.

One of the simplest dynamical processes than can be associated with a random graph is a random walk [6], describing the hopping of a system point between vertices of a graph, at each time step randomly selecting one of the neighbouring vertices as the target vertex to jump to. This process constitutes an example of a discrete Markov chain, and variants of it have been used to analyse a very broad range of phenomena, including diffusion [7], infection dynamics and the spread of diseases in social networks [8, 9], the transmission of information in communication networks (*e.g.* [10]), the dynamics of glassy systems at low temperatures as conceptualized in terms of hopping between long-lived states in state space [11–13], or the dynamics of conformational changes in macro-molecules [14]. Aspects of persistence and memory were emphasised in [15], and in the context of search algorithms [16, 17], random walks in complex networks have become the basis of multi-billion dollar industries.

As succinctly pointed out by Lovász [18], there is, in fact, "not much difference between the theory of random walks on graphs and the theory of finite Markov chains" and so it will come as no surprise that properties of random walks in complex networks have been studied in their own right [18–20] or used as a tool to analyse network structure [21].

One of the most powerful and versatile general tools to study topological properties of graphs has been Random Matrix Theory. Moments of the spectral density of the adjacency matrix of a graph or network, for instance, encode information of the number of closed walks of a given length in the system [22–24]. There is clearly a close link to random walks and diffusion [7], and properties of Laplacian spectra have indeed been advocated as providing diagnostic tools for network structure [25, 26]. The computation of spectra for ensembles of sparse random matrices was pioneered more than two decades ago by Bray and Rodgers [7, 27]. A complete evaluation of the theory appeared to be impossible, however, and approximations [24, 28–30] have been developed to obtain explicit results. Fairly complete analytic control, both for asymptotic spectra in the limit of large system sizes ($N \to \infty$) [31], and for large single instances [32] has been obtained only fairly recently.

In the present paper, we adapt the techniques developed in [31, 32] to study spectra of large Markov matrixes defined in terms of complex random graphs. Our main motivation derives from the fact that knowing the spectra of stochastic matrices is tantamount to knowing the complete spectrum of relaxation times of stochastic processes described by them. Our methods are fairly general and apply to arbitrary graph ensembles defined in terms of a configuration model, *i.e.* to graphs that are maximally random, subject only to a given degree distribution, for which we need to assume that the mean degree remains finite in the thermodynamic limit. It is worth noting at the outset, though, that systems defined on Erdős–Renyi graphs with

diverging mean degree are within easy reach of our methods. The only other restriction that we currently have to make is that the Markov matrices under investigation satisfy a detailed balance condition with an equilibrium distribution, hence that Markov chains under study are time reversible. This would apply to most physical systems, but only to a subset of technical or socio-economic systems one might be interested in.

The spectrum of fully connected Markov matrices satisfying a detailed balance condition was shown to converge to a semi-circular law [33] in the large system limit, and to a circular law, if the detailed balance condition is dropped [34]. Asymptotic results related to the circular law were obtained for Erdős–Renyi graphs with mean connectivity diverging in the thermodynamic limit in [35]. There are a number of recent results concerning spectra of graph Laplacians, which are simply related to those of Markov matrices; see *e.g.* [36–38]. However, solutions do involve mean-field [36] or large mean degree [37] approximations, or they rely on a strictly self-similar construction of the underlying graph [38]. We are not aware of general exact solutions of the spectral problem for Markov matrices or their corresponding master-equation operators for the case where the mean connectivity stays finite in the thermodynamic limit.

The remainder of this paper is organised as follows. In Sect. 2, we introduce the general framework and specify the class of systems to be analysed in what follows. Section 3 describes the calculation of spectra of sparse Markov matrices using a cavity approach. We will develop the theory separately for the case of unbiased random walks and for more general Markov matrices. Although the latter constitute a special case of the former, there are simplifications available in the case of random walk transition matrices, which are not permitted in the more general case. An alternative calculation based on the replica method will be relegated to an appendix. Section 4 will be devoted to the description of analytically tractable limiting cases which allow to obtain results for spectral densities in closed form, *viz.* the case of unbiased random walks on regular random graphs (or on Erdős–Renyi graphs in the large mean connectivity limit), as well as the limiting behaviour of spectra of more general Markov matrices in the limit of large mean connectivity (for both regular random graphs and Erdős–Renyi graphs). In Sect. 5, we present results for example cases, and we compare with simulations to assess the quality of our findings. We conclude with a summary and discussion in Sect. 6. A short summary of the main results and findings presented here has appeared elsewhere [39].

2. Markov chains and random walks on complex networks

2.1. General framework

We consider discrete Markov chains in an N-dimensional state space, described by an evolution equation for a probability vector $\boldsymbol{p}(t) = (p_i(t)) \in (\mathbb{R}^+)^N$ of the form

$$\boldsymbol{p}(t+1) = W\boldsymbol{p}(t)\,. \tag{1}$$

In order that probability vectors remain non-negative and normalized at all times, it is required that W be a stochastic matrix, with $W_{ij} \geq 0$ for all (i,j), and $\sum_i W_{ij} = 1$ for all j. These conditions entail generally that the spectrum of W is contained in the unit disc of the complex plane, $\sigma(W) \subseteq \{z; |z| \leq 1\})$. If W satisfies a detailed balance condition with an equilibrium distribution, $p_i = p_i^{\rm eq}$, such that $W_{ij}p_j = W_{ji}p_i$ for all pairs (i,j), then W can be symmetrized by a similarity transformation — $\mathcal{W}_{ij} = p_i^{-1/2} W_{ij} p_j^{1/2} = \mathcal{W}_{ji}$ — implying that the spectrum of W is real, and $\sigma(W) \subseteq [-1,1]$.

The Theorems of Perron and Frobenius [40] imply that there is exactly one eigenvalue $\lambda_1^\mu = +1$ for every irreducible component μ of state space, with all other eigenvalues satisfying $|\lambda_\alpha^\mu| \leq 1$, for $\alpha \neq 1$. If the system is free of cycles, the last inequalities are, in fact, sharp. If, moreover, the system is overall irreducible, the right eigenvector $\boldsymbol{v}_1$ corresponding to the largest eigenvalue $\lambda_1 = 1$ represents the (unique) equilibrium distribution of the system, $\boldsymbol{v}_1 = \boldsymbol{p}^{\rm eq}$, with $\boldsymbol{w}_1 = (1,\ldots,1)$ as the corresponding left eigenvector.

The relation between eigenvalues of W and the spectrum of relaxation times of the process it describes is easily understood by following the evolution of an initial probability vector $\boldsymbol{p}(0)$ over t time steps, *i.e.* by evaluating $\boldsymbol{p}(t) = W^t\boldsymbol{p}(0)$. Assuming the system to be overall irreducible, one obtains

$$\boldsymbol{p}(t) = \boldsymbol{p}^{\rm eq} + \sum_{\alpha(\neq 1)} \lambda_\alpha^t \; \boldsymbol{v}_\alpha \;\; (\boldsymbol{w}_\alpha, \boldsymbol{p}(0)) \tag{2}$$

in terms of a spectral decomposition of W, where we have used that $\lambda_1 = 1$, and where $\boldsymbol{v}_\alpha$ and $\boldsymbol{w}_\alpha$ are the right and left eigenvectors of W, respectively, with $\boldsymbol{v}_1$ corresponding to the equilibrium distribution as mentioned above. If the system is free of cycles, relaxation to equilibrium is exponential (as long as the system size N is finite), with relaxation times related to eigenvalues via

$$\tau_\alpha = -\frac{1}{\ln|\lambda_\alpha|}\,, \qquad \alpha \neq 1\,. \tag{3}$$

We are interested in the behaviour of Markov chains for large N, and specifically in Markov transition matrices describing stochastic dynamics in complex systems. We construct them in terms of unnormalized transition

matrices $\Gamma = (\Gamma_{ij}) = (c_{ij}K_{ij})$, in which $c = (c_{ij})$ with $c_{ij} \in \{0,1\}$ denotes a symmetric connectivity matrix that specifies a network of *possible* transitions, while the edge weights K_{ij} encode their relative strengths by setting

$$W_{ij} = \begin{cases} \frac{\Gamma_{ij}}{\Gamma_j}\,, & i \neq j\,, \\ 1\,, & i = j \text{ and } k_j = 0\,, \end{cases} \tag{4}$$

where

$$\Gamma_j = \sum_i \Gamma_{ij} \tag{5}$$

and $k_j = \sum_i c_{ij}$ denotes the degree of vertex j. The above construction associates an irreducible component of the Markov chain with each distinct cluster, and thus in particular also with each of the isolated sites in the graph.

A closely related operator is the corresponding master-equation operator

$$M_{ij} = \begin{cases} \frac{\Gamma_{ij}}{\Gamma_j}\,, & i \neq j\,, \\ -1\,, & i = j \text{ and } k_j \neq 0\,, \\ 0\,, & \text{otherwise}\,, \end{cases} \tag{6}$$

in terms of which we have the continuity equation

$$p_i(t+1) - p_i(t) = \sum_j [W_{ij}p_j(t) - W_{ji}p_i(t)] = \sum_j M_{ij}p_j(t)\,. \tag{7}$$

Taking for simplicity the unnormalized transition matrices $\Gamma = (\Gamma_{ij})$ to be symmetric to begin with, the equilibrium distribution[1] corresponding to W is $p_i = p_i^{\mathrm{eq}} = \frac{\Gamma_i}{\mathcal{Z}}$, so that the corresponding symmetrized Markov matrices take the form

$$\mathcal{W}_{ij} = p_i^{-1/2} W_{ij} p_j^{1/2} = \frac{\Gamma_{ij}}{\sqrt{\Gamma_i \Gamma_j}} \tag{8}$$

for $\Gamma_{ij} > 0$, hence $\Gamma_i > 0$ and $\Gamma_j > 0$, and $\mathcal{W}_{ii} = 1$ for isolated sites.

This is the point to note that, while (4), (5) may be thought of as a 'natural' way of constructing random Markov matrices in terms of complex networks, random Markov matrices defined on complete graphs have alternatively been constructed by taking squared moduli of elements of random

[1] This construction is unique only for systems that are irreducible. For systems with several irreducible components (including those with isolated sites), an equilibrium distributions of this structure can be constructed for each irreducible component, and any convex combination of these is a valid equilibrium distribution for the entire system.

orthogonal or random unitary matrices. Due to the orthogonality or unitarity constraints, these matrices are, however always *bistochastic*, *i.e.* both column sums and row sums are normalized to one. Ensembles of such matrices have been discussed, for instance, in the context of quantum graphs [41]. Their spectral properties were looked at in [42], while ways of generating them efficiently as well as properties of the probability measure of the ensemble of these matrices over the Birkhoff polytope were investigated in [43].

2.2. Unbiased random walks

It is worthwhile to record the main identities for the important special case of unbiased random walks. In this case, the edge-weights are uniform, $K_{ij} = 1$, so that transitions to neighbouring vertices with equal probability. This gives rise to

$$W_{ij} = \begin{cases} \frac{c_{ij}}{k_j}\,, & i \neq j\,, \\ 1\,, & i = j \text{ and } k_j = 0\,, \end{cases} \tag{9}$$

in which $k_j = \sum_i c_{ij}$ is the degree of vertex j. The corresponding master-equation operator is

$$M_{ij} = \begin{cases} \frac{c_{ij}}{k_j}\,, & i \neq j\,, \\ -1\,, & i = j \text{ and } k_j \neq 0\,, \\ 0\,, & \text{otherwise}\,. \end{cases} \tag{10}$$

The equilibrium distribution in the present case is $p_i = \frac{k_i}{\mathcal{Z}}$, and the symmetrized version of the Markov matrix takes the form

$$\mathcal{W}_{ij} = \begin{cases} \frac{c_{ij}}{\sqrt{k_i k_j}}\,, & i \neq j\,, \\ 1\,, & i = j \text{ and } k_j = 0\,. \end{cases} \tag{11}$$

The symmetrized master equation operator in this case is the so-called normalized graph Laplacian

$$\mathcal{L}_{ij} = \begin{cases} \frac{c_{ij}}{\sqrt{k_i k_j}}\,, & i \neq j\,, \\ -1\,, & i = j \text{ and } k_j \neq 0\,, \\ 0\,, & \text{otherwise}\,. \end{cases} \tag{12}$$

Our calculation of spectra below will be performed for Markov matrices, assuming that they satisfy a detailed balance condition, and hence can be symmetrized by a similarity transformation as described above. The spectra of the corresponding master-equation operators are related to those of the Markov matrices through a simple shift by -1.

3. Spectra of Markov matrices

To compute spectra of the random Markov matrices introduced above, we follow Edwards and Jones [44] and express the resolvent identity

$$\rho_W(\lambda) = \frac{1}{\pi N} \lim_{\varepsilon\to 0} \operatorname{Im} \operatorname{Tr} \left[\lambda_\varepsilon \mathbb{I} - W\right]^{-1} , \qquad \lambda_\varepsilon = \lambda - i\varepsilon \tag{13}$$

for the spectral density $\rho_W(\lambda)$ of the stochastic matrix W in terms of a derivative

$$\rho_W(\lambda) = -\lim_{\varepsilon\to 0} \frac{2}{\pi N} \operatorname{Im} \frac{\partial}{\partial \lambda} \log Z_W(\lambda) \tag{14}$$

of the logarithm of the Gaussian integral

$$Z_W(\lambda) = \int \prod_{i=1}^{N} \frac{du_i}{\sqrt{2\pi/i}} \exp\left\{ -\frac{i}{2} \sum_{i,j} \left(\lambda_\varepsilon \delta_{ij} - \mathcal{W}_{ij}\right) u_i u_j \right\} . \tag{15}$$

Here, $\mathcal{W}$ is the symmetrized version of W, obtained via a similarity transform that involves the equilibrium distribution $\boldsymbol{p}^{\mathrm{eq}}$ as discussed above. The representation (14), (15) expresses the spectral density as a sum over "single site variances"

$$\rho_W(\lambda) = \operatorname{Re} \frac{1}{\pi N} \sum_i \left\langle u_i^2 \right\rangle \tag{16}$$

of the complex Gaussian measure

$$P_W(\boldsymbol{u}) = \frac{1}{Z_W} \exp\left\{ -\frac{i}{2} \sum_{i,j} \left(\lambda_\varepsilon \delta_{ij} - \mathcal{W}_{ij}\right) u_i u_j \right\} . \tag{17}$$

Here and in the following, we shall omit explicitly writing the $\lim_{\varepsilon\to 0}$, and take it to be implied.

At this point, there are two principal ways to proceed. One can move directly to computing the non-random density of states for the thermodynamic limit $N \to \infty$ of a given system by averaging Eq. (14) over the ensemble of Markov matrices in question, using the replica method to perform averages as proposed in [44], and appropriately adapting the sparse matrix techniques developed in [31]. We will present this calculation in an appendix. Alternatively, one can use the cavity approach proposed in [32] to evaluate the single instance spectral density in terms of variances of single-site marginals, as in (16). In the thermodynamic limit, recursion relations for the cavity variances obtained within that approach can be interpreted as stochastic recursions, allowing to formulate self-consistency relations for their distributions, which are found to be equivalent to those obtained using replica. This is the approach we shall describe here.

In order to compute the single-site marginals of (17) required to evaluate $\rho_W(\lambda)$ according to (16), we need to distinguish between single-site marginals on isolated sites and those for sites that are not isolated. Referring to the structure of $\mathcal{W}$, we find single-site marginals on isolated sites to be of the form

$$P_i^{\rm is}(u_i) \propto e^{-\frac{i}{2}(\lambda_\varepsilon - 1)\, u_i^2}\,. \tag{18}$$

On the non-isolated sites, we perform a transformation of variables, $\frac{u_i}{\sqrt{\Gamma_i}} \to u_i$. In terms of the transformed variables, we have

$$\rho_W(\lambda) = p_N(0)\delta(\lambda - 1) + {\rm Re}\,\frac{1}{\pi N}\sum_i \Gamma_i \left\langle u_i^2 \right\rangle\,, \tag{19}$$

with $p_N(0) = \frac{N^{\rm is}}{N}$ denoting the fraction of isolated sites, and only non-isolated sites with $\Gamma_i > 0$ contributing to the second sum.

The marginal $P_i(u_i)$ of a (transformed) variable on a non-isolated site can be expressed in terms of joint cavity marginal $P^{(i)}(\boldsymbol{u}_{\partial i})$ of the degrees of freedom on sites in the neighbourhood ∂i of i as

$$P_i(u_i) \propto e^{-\frac{i}{2}\Gamma_i\lambda_\varepsilon\, u_i^2} \int d\boldsymbol{u}_{\partial i}\; e^{i\sum_{j\in\partial i} K_{ij}u_iu_j}\, P^{(i)}(\boldsymbol{u}_{\partial i})\,. \tag{20}$$

If i were the root of a tree-graph, the joint cavity marginal $P^{(i)}(\boldsymbol{u}_{\partial i})$ would factor

$$P^{(i)}(\boldsymbol{u}_{\partial i}) = \prod_{j\in\partial i} P_j^{(i)}(u_j) \tag{21}$$

in terms of single-site cavity marginals on sites adjacent to i. While this kind of factorization is only approximate on a locally tree-like graph, it becomes asymptotically exact for finitely coordinated graphs in the thermodynamic limit. For sufficiently large graphs then, the integration over degrees of freedom in the neighbourhood of i can be taken to factor, and be expressed in terms of single-site cavity marginals as

$$P_i(u_i) \propto e^{-\frac{i}{2}\Gamma_i\lambda_\varepsilon\, u_i^2} \prod_{j\in\partial i} \int du_j\, e^{iK_{ij}u_iu_j}\, P_j^{(i)}(u_j)\,. \tag{22}$$

By the same line of reasoning, the single-site cavity marginals themselves satisfy a set of self-consistency equations given by

$$P_j^{(i)}(u_j) \propto e^{-\frac{i}{2}\Gamma_j\lambda_\varepsilon\, u_j^2} \prod_{\ell\in\partial j\setminus i} \int du_\ell\, e^{iK_{j\ell}u_ju_\ell}\, P_\ell^{(j)}(u_\ell)\,. \tag{23}$$

These relations are exact on trees; for finitely connected random graphs they become asymptotically exact in the thermodynamic limit. A moment of reflection shows that they are solved [32] by complex Gaussians of the form

$$P_j^{(i)}(u_j) = \sqrt{\frac{\omega_j^{(i)}}{2\pi}} \ \exp\left\{-\frac{1}{2}\omega_j^{(i)} u_j^2\right\}, \tag{24}$$

with $\mathrm{Re}\,\omega_j^{(i)} \geq 0$, entailing that the inverse cavity variances satisfy the self-consistency equations

$$\omega_j^{(i)} = i\lambda_\varepsilon \, \Gamma_j + \sum_{\ell \in \partial j \setminus i} \frac{K_{j\ell}^2}{\omega_\ell^{(j)}} \,. \tag{25}$$

These can be solved iteratively on large single instances. Single-site marginals, too, will be Gaussian with inverse variances expressed in terms of solutions of (25) as

$$\omega_i = i\lambda_\varepsilon \, \Gamma_i + \sum_{j \in \partial i} \frac{K_{ij}^2}{\omega_j^{(i)}} \,. \tag{26}$$

In terms of these inverse variances of single-site marginals then, we have

$$\rho_W(\lambda) = p_N(0)\delta(\lambda - 1) + \mathrm{Re}\,\frac{1}{\pi N} \sum_i \frac{\Gamma_i}{\omega_i} \,. \tag{27}$$

In the limit of infinite system size, Eqs. (25) can be read as stochastic recursions for the set of inverse cavity variances, with randomness generated by the random environment of each bond (i, j) in the system. Yet, it turns out that a straightforward derivation of a self-consistency equation for the probability density function $\pi(\omega)$ of inverse cavity variances from Eqs. (25) is possible only for the case of unbiased random walks on complex networks. In all other cases, correlations (beyond degree) between Γ_j and the $K_{j\ell}$ on the r.h.s. of (25) prevent straightforward averaging over the graph ensemble, and a slight modification of the analysis is required, which will be described below.

Unbiased random walks: In the case of unbiased random walks, however, we can proceed directly from Eqs. (25). In this case, we have $K_{ij} \equiv 1$, hence $\Gamma_j = k_j$ and $\mathcal{W}_{ij} = \frac{c_{ij}}{\sqrt{k_i k_j}}$ for non-isolated sites, where k_i and k_j are degrees of vertices i and j.

A self-consistency equation for $\pi(\omega)$ is then obtained from (25) by observing that the $\omega_\ell^{(j)}$ for the vertices ℓ incident on j appearing on the r.h.s of

(25) are in the thermodynamic lime *independently* drawn from $\pi(\omega)$. Noting that the probability for a site i to be connected to a site j with coordination $k_j = k$ and thus $\Gamma_j = k$ is given by $p(k)k/c$, one obtains an integral equation for a probability density function $\pi(\omega)$ for inverse cavity variances of the form

$$\pi(\omega) = \sum_{k\geq 1} p(k) \frac{k}{c} \int \prod_{\nu=1}^{k-1} d\pi(\omega_\nu)\ \delta(\omega - \Omega_{k-1}) \tag{28}$$

in which

$$\Omega_{k-1} = \Omega\left(\{\omega_\nu\}_{\nu=1}^{k-1}\right) = i\lambda_\varepsilon k + \sum_{\nu=1}^{k-1} \frac{1}{\omega_\nu}\,. \tag{29}$$

In terms of the solution of (28), one obtains the spectral density of W for a random graph with degree distribution $p(k)$ as

$$\rho(\lambda) = p(0)\delta(\lambda - 1) + \frac{1}{\pi}\,\mathrm{Re} \sum_{k\geq 1} p(k) \int \prod_{\nu=1}^{k} d\pi(\omega_\nu)\ \frac{k}{i\lambda_\varepsilon k + \sum_{\nu=1}^{k} \frac{1}{\omega_\nu}}\,. \tag{30}$$

As explained in [31], the solution of (28) allows to disentangle contributions related to the density of *localized* and *extended* states, respectively. The former are related to a singular contribution to $\pi(\omega)$ with support on the imaginary axis, whereas the contribution to the latter corresponds to a regular contribution to $\pi(\omega)$ with support in $\mathrm{Re}\,\omega > 0$.

General Markov matrices: In order to deal with correlations between Γ_j and the $K_{j\ell}$ in (25) for Markov processes other than the unbiased random walk, we return to the Gaussian measure (17) in terms of which the problem was originally formulated, and rewrite it — inserting the original definition of the Γ_j and using transformed variables on non-isolated sites — as

$$\begin{aligned} P_W(\boldsymbol{u}) \;=\; & \frac{1}{Z_W} \exp\left\{ -\frac{i}{2} \sum_{i,\mathrm{isolated}} (\lambda_\varepsilon - 1) u_i^2 \right. \\ & \left. + \frac{i}{2} \sum_{i,j} c_{ij} \left[\frac{1}{2}\lambda_\varepsilon K_{ij} \left(u_i^2 + u_j^2\right) - K_{ij}\ u_i u_j \right] \right\}. \end{aligned} \tag{31}$$

In terms of this reformulation, the expression for single-site marginals in terms of single-site cavity marginals, and the recursion relation for single-

site cavity marginals now read

$$P(u_i) \propto \prod_{j\in\partial i} \int du_j \, \exp\left\{-\frac{i}{2}\lambda_\varepsilon \sum_{j\in\partial i} K_{ij}\left(u_i^2+u_j^2\right) + i\sum_{j\in\partial i} K_{ij}\; u_i u_j\right\} P_j^{(i)}(u_j) \tag{32}$$

and

$$P_j^{(i)}(u_j) \propto \prod_{\ell\in\partial j\setminus i} \int du_\ell \, \exp\left\{-\frac{i}{2}\lambda_\varepsilon K_{j\ell}\left(u_j^2+u_\ell^2\right) + iK_{j\ell}\; u_j u_\ell\right\} P_\ell^{(j)}(u_\ell)\,, \tag{33}$$

respectively. The modified set of cavity recursions, too, is self-consistently solved by complex Gaussians of the form (24), giving rise to the following reformulated recursion for inverse variances of cavity marginals,

$$\omega_j^{(i)} = \sum_{\ell\in\partial j\setminus i}\left(i\lambda_\varepsilon K_{j\ell} + \frac{K_{j\ell}^2}{\omega_\ell^{(j)} + i\lambda_\varepsilon K_{j\ell}}\right)\,. \tag{34}$$

This version allows ensemble averaging in the thermodynamic limit, following the line of reasoning presented above for the unbiased random walk case, as contributions to the r.h.s. of (34) are now independent. One obtains a self-consistency equation for the distribution $\pi(\omega)$ of inverse cavity variances which is structurally very similar to (28), *viz.*

$$\pi(\omega) = \sum_{k\geq 1} p(k)\frac{k}{c}\int \prod_{\nu=1}^{k-1} d\pi(\omega_\nu)\; \langle\delta(\omega-\Omega_{k-1})\rangle_{\{K_\nu\}}\,, \tag{35}$$

where now

$$\Omega_{k-1} = \Omega\left(\{\omega_\nu, K_\nu\}_{\nu=1}^{k-1}\right) = \sum_{\nu=1}^{k-1}\left(i\lambda_\varepsilon K_\nu + \frac{K_\nu^2}{\omega_\nu + i\lambda_\varepsilon K_\nu}\right)\,, \tag{36}$$

and where $\langle\ldots\rangle_{\{K_\nu\}}$ in (35) denotes an average over the distribution of a set of (independent) edge weights. In terms of its solution, the spectral density in the thermodynamic limit is given by

$$\rho(\lambda) = p(0)\delta(\lambda-1) + \frac{1}{\pi}\,\mathrm{Re}\sum_{k\geq 1} p(k)\int\prod_{\nu=1}^{k} d\pi(\omega_\nu)\;\left\langle \frac{\sum_{\nu=1}^k K_\nu}{\sum_{\nu=1}^k\left(i\lambda_\varepsilon K_\nu + \frac{K_\nu^2}{\omega_\nu+i\lambda_\varepsilon K_\nu}\right)}\right\rangle_{\{K_\nu\}}\,. \tag{37}$$

4. Analytically tractable limiting cases

There are a few cases where it is possible to obtain results analytically and in closed form. These are the unbiased random walk problem on random regular graphs and the random walk problem on Erdős–Renyi graphs in the large mean connectivity limit. For more general Markov matrices, large c-approximations can be formulated for random regular and Erdős–Renyi graphs which become exact in the $c \to \infty$ limit.

The solution of the unbiased random walk problem on a regular random graph with degree distribution $p(k) = \delta_{k,c}$ starts with the observation that each node of a random regular graph is equivalent, and so is the environment of every node (and every link). One would, therefore, expect that Eq. (28) is solved by a δ-function, $\pi(\omega) = \delta(\omega - \bar{\omega})$. Indeed, this ansatz solves (28) and gives rise to a quadratic self-consistency equation

$$\bar{\omega} = i\lambda_\varepsilon c + \frac{c-1}{\bar{\omega}} \tag{38}$$

for the parameter $\bar{\omega}$. Its solution, when inserted into (30), gives a closed-form expression for the spectral density of the form

$$\rho(\lambda) = \frac{c}{2\pi} \frac{\sqrt{4\frac{c-1}{c^2} - \lambda^2}}{1-\lambda^2}\,. \tag{39}$$

This expression is readily recognised as a variant of the Kesten–McKay distribution for the eigenvalue density of adjacency matrices of regular random graphs [45], adapted to capture the spectral problem of the Markov transition matrix for an unbiased random walk.

The same result provides an accurate approximate description also for Erdős–Renyi random graphs at large mean degree c, for which the degree distribution becomes sharply peaked at the mean degree c. The approximation becomes asymptotically exact as $c \to \infty$, where fluctuations of the degree distribution become negligible relative to the mean, and (39) approaches a semicircular law for rescaled eigenvalues $\mu = \lambda/\sqrt{c}$, *viz.*

$$\rho(\mu) = \frac{1}{2\pi}\sqrt{4-\mu^2}\,, \tag{40}$$

as $c \to \infty$.

A similar line of reasoning allows to obtain the spectral density for more general Markov matrices on Erdős–Renyi and random regular graphs in the large c limit. Noting that in both cases one can refer to the law of large numbers (LLN), allowing to replace Ω_{k-1} in (36) by a sum of averages, one expects the ansatz $\pi(\omega) = \delta(\omega - \bar{\omega})$ to provide an accurate approximate

solution to (35). The ansatz gives rise to a self-consistency equation for the parameter $\bar{\omega}$ of the form

$$\bar{\omega} \simeq c \left[i\lambda_\varepsilon \langle K \rangle + \left\langle \frac{K^2}{\bar{\omega} + i\lambda_\varepsilon K} \right\rangle \right] . \tag{41}$$

This equation is easily solved numerically. In terms of its solution $\bar{\omega}$, one can once more invoke the LLN in the expression for the spectral density to obtain

$$\rho(\lambda) = \frac{1}{\pi} \mathrm{Re} \left[\frac{\langle K \rangle}{i\lambda_\varepsilon \langle K \rangle + \left\langle \frac{K^2}{\bar{\omega} + i\lambda_\varepsilon K} \right\rangle} \right] = \frac{1}{\pi} \mathrm{Re} \left[\frac{c\langle K \rangle}{\bar{\omega}} \right] . \tag{42}$$

Note that this requires (and entails self-consistently) that $\bar{\omega} \propto \langle K \rangle$ for the spectral density to be independent of the K-scale. Moreover, for large c, we have $\bar{\omega} \sim c$ which allows to approximate (41) by a quadratic equation; its solution, when inserted into the final equation for the spectral density, gives rise to a Wigner semi-circular distribution of the form

$$\rho(\lambda) = \frac{c}{2\pi} \frac{\langle K \rangle^2}{\langle K^2 \rangle} \sqrt{\frac{4\langle K^2 \rangle}{c\langle K \rangle^2} - \lambda^2} \, . \tag{43}$$

This expression, too, is invariant under rescaling of the edge weights K_{ij} as it should, because K scales are immaterial in normalized Markov transition matrices. As in the case of unbiased random walks, a $c \to \infty$ limit exists for the distribution of rescaled eigenvalues $\mu = \lambda/\sqrt{c}$, and takes the form

$$\rho(\mu) = \frac{1}{2\pi} \frac{\langle K \rangle^2}{\langle K^2 \rangle} \sqrt{\frac{4\langle K^2 \rangle}{\langle K \rangle^2} - \mu^2} \, . \tag{44}$$

In the large c limit, therefore, eigenvalue densities of random Markov matrices defined in terms of Erdős–Renyi or random regular graphs are given by Wigner semi-circular laws, with spectral radius fully determined by first and second moments of the weight distribution. The result (44) is expected to describe the density of rescaled eigenvalues in the large mean connectivity limit ($c \to \infty$) for *any* degree distribution for which relative fluctuations of degree become asymptotically negligible compared to the value of the mean degree c, as the large c limit is taken.

5. Results

In what follows, we report results for a number of different ensembles of sparse Markov matrices. The variety of possible realisations to which

our theory could, in principle, apply is clearly far too large to even attempt giving anything approaching an overview, so we restrict ourselves to a set of examples chosen to illustrate the working of our approach and the quality of the results obtainable. Examples are deliberately chosen to complement those given in an earlier short account of the theory [39].

Where analytic results are compared with simulation results obtained by numerical diagonalization of finite dimensional matrices, we usually use a set of 1000×1000 matrices, averaging spectra over a sample of 5000 matrices, randomly drawn from the ensembles under study.

In Figs. 1 and 2, we look at spectra of Markov matrices describing unbiased random walks on sparse graphs with power-law degree distribution of the form $p(k) \propto k^{-\gamma}$, choosing a lower cut-off of $k_{\min} = 2$ for the degrees, entailing that there will not be any isolated sites in these systems. Figure 1 looks at the case $\gamma = 3$, Fig. 2 at $\gamma = 4$.

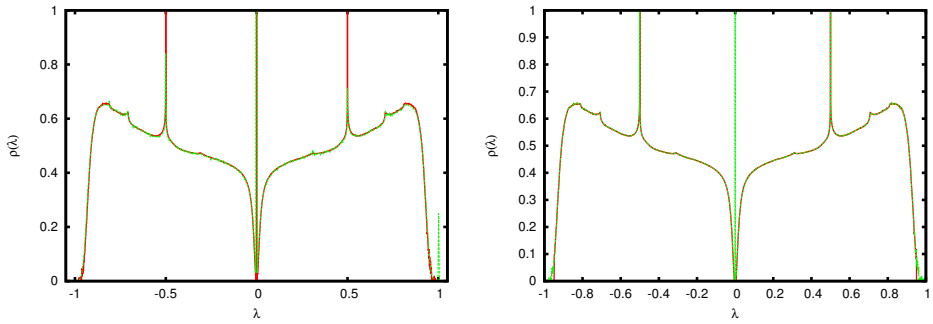

Fig. 1. (Colour online) Spectral density of the transition matrix for an unbiased random walk on a random graph with power-law degree distribution $p(k) \propto k^{-3}$, with $k \geq k_{\min} = 2$. Left panel: analytic results for the full density of states obtained by solving (28) via population dynamics (full red curve) compared with simulation results for an ensemble of 1000×1000 matrices (dashed green curve). Curves are virtually on top of each other. Right panel: analytic results separately exhibiting the density of extended states (full red curve) and total density of states (dashed green curve). Except in the immediate vicinity of $\lambda = \pm 1$ curves are virtually on top of each other.

In the $\gamma = 3$ case in the right panel of Fig. 1, one can discern mobility edges at $\lambda_c \simeq \pm 0.950$ on the scale of the figure as shown, separating extended state at $|\lambda| \leq |\lambda_c|$ from localized states at $|\lambda| > |\lambda_c|$. In addition, there is also a narrow gap in the density of extended states at small $|\lambda|$, *viz.* for $-0.004 \lesssim \lambda \lesssim 0.004$ (not discernible on the scale of the figure) with only localized states existing in the gap.

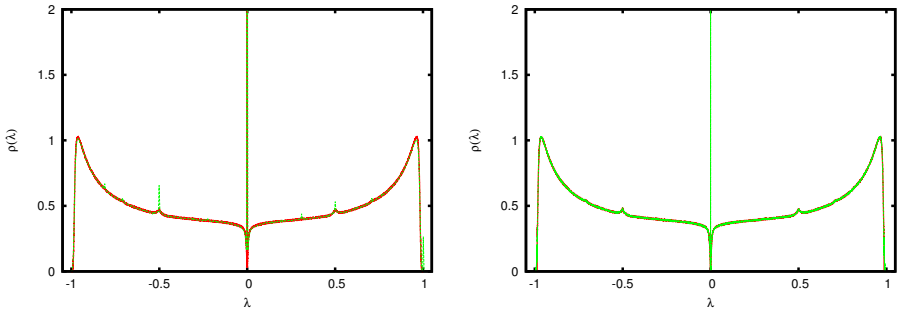

Fig. 2. (Colour online) Spectral density of the transition matrix for an unbiased random walk on random graph with power-law degree distribution $p(k) \propto k^{-4}$, with $k \geq k_{\min} = 2$. Left panel: analytic results for the full density of states obtained by solving (28) via population dynamics (full red curve) compared with simulation results (dashed green curve). Curves are virtually on top of each other. Right panel: analytic results separately exhibiting the density of extended states (full red curve) and total density of states (dashed green curve). Curves are virtually on top of each other (see the main text for details).

As explained in detail in [31], the distinguishing feature of the localized states is that they correspond to a singular contribution to the solution $\pi(\omega)$ of (28), with support on the imaginary axis. To reveal this contribution, the spectral density (30) needs to be evaluated with a small non-zero regularizing ε; in the present paper, unless otherwise specified, we choose $\varepsilon = 10^{-4}$ for this purpose.

In the $\gamma = 4$ case shown in Fig. 2, one would have to zoom into the $\lambda \simeq \pm 1$ regions to reveal mobility edges at $\lambda_c \simeq \pm 0.987$, and into the small $|\lambda|$ region to exhibit an even narrower gap in the density of extended states for $-0.0014 \lesssim \lambda \lesssim 0.0014$, with once more only localized states existing in the gap, as in the $\gamma = 3$ case.

The agreement between analytic and simulation results in both cases is excellent. In the $\gamma = 4$ case, there are a few small peaks that can be observed in the simulation, mainly at $\lambda = \pm 0.5$ and $\lambda = \pm\sqrt{2}/2$ and at $\lambda = 1$ which are absent or appear as cusps in the analytic results for the thermodynamic limit. These are due to finite-size effects affecting the simulation results *e.g.* the peaks at $\lambda = \pm 0.5$ and at $\lambda = 1$ are mainly due to isolated 3-cycles, which are suppressed in the limit $N \to \infty$.

In Fig. 3, we present results for systems with unnormalized transition matrix elements taking the form of Kramers transition rates

$$\Gamma_{ij} = c_{ij} e^{-\beta(V_{ij} - E_j)} \,. \tag{45}$$

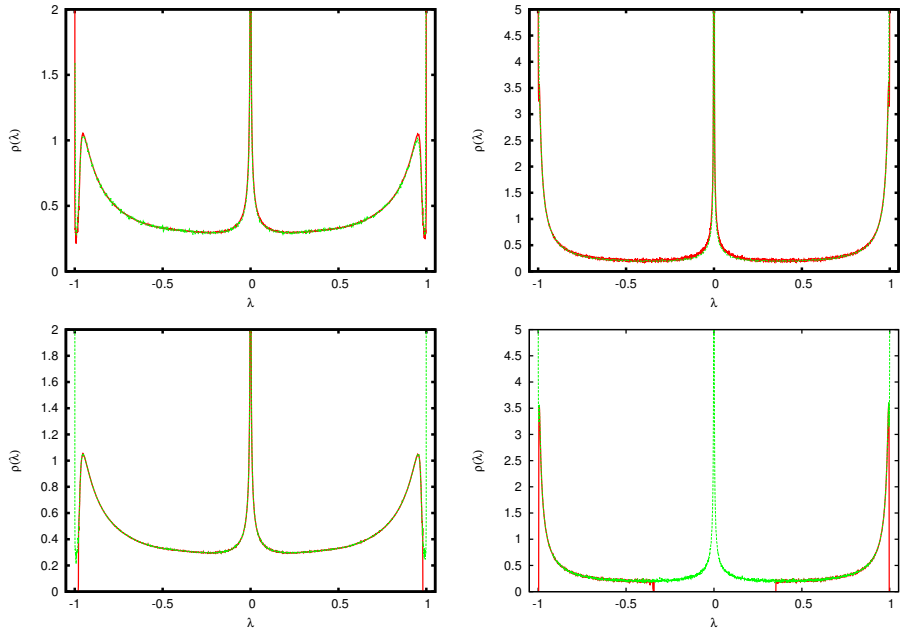

Fig. 3. (Colour online) Spectral density of transition matrices with Kramers transition rates as described in the main text, with $\beta = 2$ (left set of panels) and $\beta = 5$ (right set of panels), on an Erdős–Renyi graph of mean coordination $c = 3$; note the different vertical scales. The upper row compares analytic results for the total density of states obtained via population dynamics (full red curves) with simulation results (dashed greed curves). Curves are virtually on top of each other. In the second row, we display results separately for the extended states (full red curves), and the total density of states (dashed green curves). While there are mobility edges near $\lambda = \pm 1$ for both values of the inverse temperature, we see a large gap in the density of extended states appearing in the $\beta = 5$ system, which is not present in the $\beta = 2$ case.

For the present study, we assume that the distribution of barrier heights $V_{ij} \geq 0$ is itself a Gibbs distribution at inverse temperature β_0, $p(V) = \beta_0 e^{-\beta_0 V}$, which could describe the influence of a *preparation*-temperature of the glassy system on the distribution of barrier heights it would exhibit. The distribution of initial energies is, in fact, arbitrary, as initial energies cancel in properly normalized stochastic matrices, so that $W_{ij} = c_{ij} e^{-\beta V_{ij}} / \sum_i c_{ij} e^{-\beta V_{ij}}$. Note that with these specifications, we get a power-law distribution of edge weights of the form

$$p(K) = \frac{\beta_0}{\beta} K^{\frac{\beta_0}{\beta} - 1}, \qquad K \in [0, 1]. \tag{46}$$

As this distribution depends only on the ratio $\frac{\beta_0}{\beta}$ of inverse temperatures characteristic of the preparation process and that prevalent when the relaxation process is observed, we can take $\beta_0 = 1$ without loss of generality. Systems of this type were studied within a heterogeneous mean-field approximation to dynamics in [13], generalizing earlier work [11, 12] to include barrier height distributions and incompletely connected networks of traps.

Figure 3 shows results for a system on an Erdős–Renyi graph of mean coordination $c = 3$, for two values of the inverse temperature, $\beta = 2$ and $\beta = 5$. Once more, theory and simulation are in excellent agreement. In this case, a substantial gap in the density of extended states appears in the centre of the spectrum for the system with the larger value of $\beta = 5$, which is absent in the $\beta = 2$ system. Attempts at a direct verification of this finding based on a numerical study of inverse participation ratios resulted only in a qualitative confirmation, as the dynamical range of matrix elements in this situation was very large, entailing that only rather small systems ($N \lesssim 250$) could be studied numerically, with EISPACK diagonalization routines failing to find eigenvectors for the larger systems, thus preventing a scaling analysis of IPRS that would include sufficiently large system sizes to be conclusive. We, therefore, looked at level-spacing distributions as an alternative. The expectation would be that level-spacing distributions would significantly deviate from the Wigner distribution $P_{\mathrm{GOE}}(s) = \frac{\pi}{2}\, e^{-\frac{\pi}{4}s^2}$, and be closer to an exponential distribution $P(s) = e^{-s}$ if a substantial fraction of states were localized. This is indeed what we find, as demonstrated in Fig. 4.

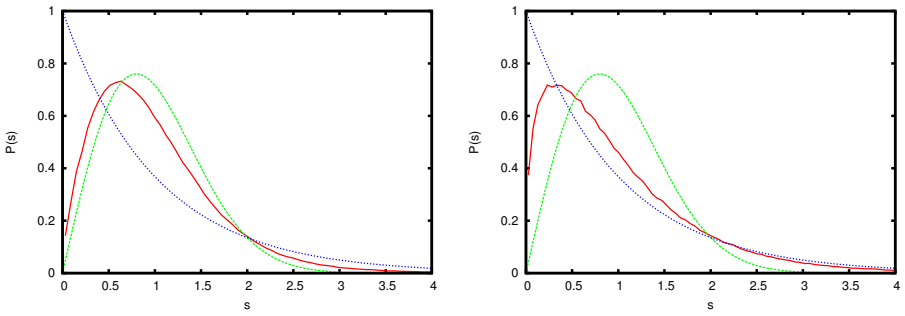

Fig. 4. (Colour online) Distribution of level spacings of transition matrices with Kramers transition rates at $\beta = 2$ (left panel) and $\beta = 5$ (right panel). Other specifications are as in Fig. 3. Level spacing distributions (full red curves) are obtained as simulation results, and compared with the Wigner surmise for GOE matrices (dashed green curves) and a Poisson distribution of level spacings (dashed blue curve) one would expect if all states were localized.

Figure 5 is devoted to testing our results about analytically tractable limiting cases, discussed in Sec. 4. It shows a comparison of the prediction (39) for the eigenvalue density of Markov transition matrices for unbiased random walks on random regular graphs, here for the case of coordination $c = 4$, and it tests the validity of that prediction for Erdős–Renyi graphs in the large c limit, by looking at a system with $c = 100$, comparing the analytic prediction (39) with results obtained by solving the self-consistency equation (28) numerically for these cases. The agreement is found to be perfect. For a test of the approximation (41), (42) valid for general Markov matrices defined on random regular graphs or Erdős–Renyi graphs at large mean connectivity c, we refer to [39].

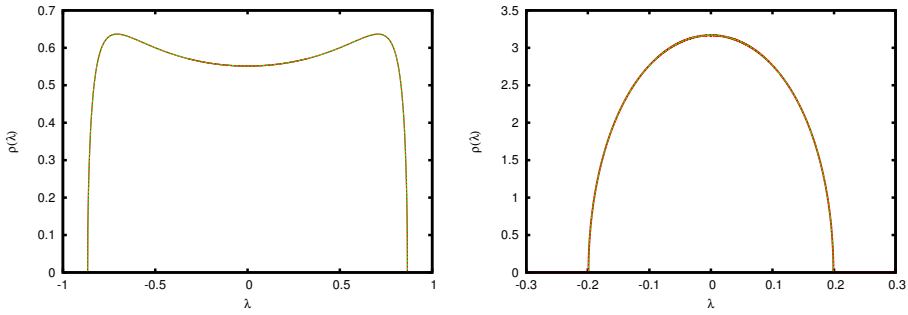

Fig. 5. (Colour online) Comparison of the closed form analytic prediction of Eq. (39) for the spectral density of the transition matrix for an unbiased random walk on a random regular graph of coordination $c = 4$ (left panel) and an Erdős–Renyi graph of mean coordination $c = 100$. Shown are results obtained by solving (28) via population dynamics (full red curves) and the predictions of Eq. (39) for $c = 4$ and $c = 100$ (dashed green curves), respectively. Curves are virtually on top of each other.

Let us, finally, turn to relaxation-time distributions for stochastic processes defined on complex networks. Getting access to them via a computation of spectra of random Markov matrices was, after all, one of the main motivations for the present project.

Indeed, given the relation Eq. (3) between eigenvalues of a transition matrix and relaxation times of the stochastic process it describes, one can translate spectral densities into spectra of relaxation times. Using the notation ρ_λ and ρ_τ to distinguish eigenvalue densities and relaxation time distributions, we have

$$\rho_\tau(\tau) = \left[\rho_\lambda\left(e^{-1/\tau}\right) + \rho_\lambda\left(-e^{-1/\tau}\right)\right] \frac{e^{-1/\tau}}{\tau^2} \,. \tag{47}$$

In Fig. 6, we look at the relaxation time distribution for a stochastic system with unnormalized Kramers transition rates of the form (45), defined on random graphs with power-law degree distribution $p(k) \propto k^{-3}$, with $k \geq k_{\min} = 2$, and a Gibbs distribution for the barrier height as used above in Fig. 3. In the figure, we also show the eigenvalue distributions giving rise to these relaxation-time spectra. With reference to Eq. (47), we note that the short relaxation times are generated by eigenvalues in the immediate vicinity of $\lambda = 0$, whereas eigenvalues very close to $\lambda = \pm 1$ correspond to the large relaxation times. Being able to disentangle extended and localized states allows us to make an analogous distinction between relaxation times corresponding to extended and to localized modes, with — in the present example — both the very fast and the very slow processes corresponding to localized modes.

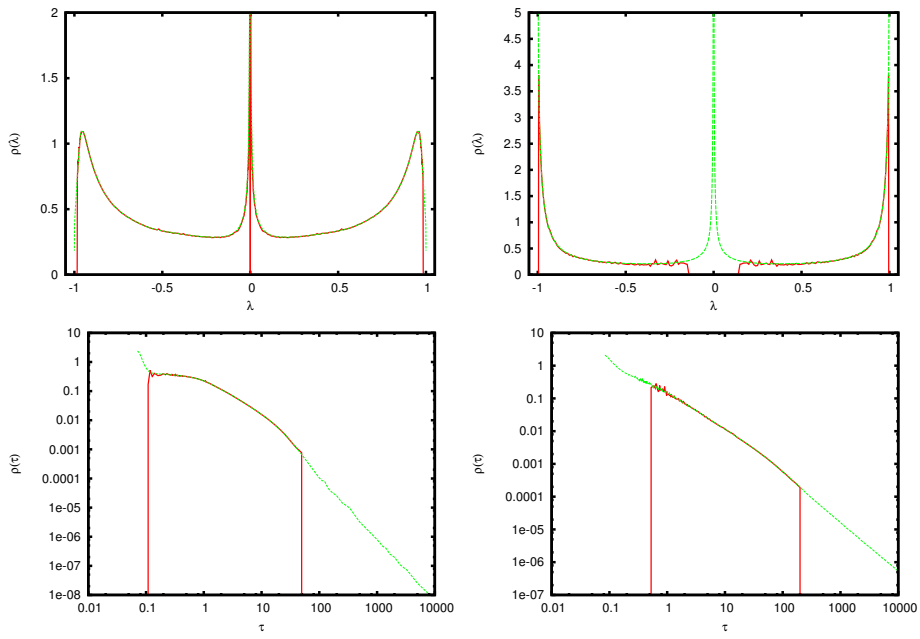

Fig. 6. (Colour online) Spectral density of transition matrices with Kramers transition rates as described in the main text (upper set of panels), and the resulting distribution of relaxation times (lower set of panels), with $\beta = 2$ (left) and $\beta = 5$ (right). The underlying graphs are chosen to have a power-law degree distribution $p(k) \propto k^{-3}$, with $k \geq k_{\min} = 2$. Both, spectra and relaxation time distributions are shown separately for the extended states (full red curves), and for the total density of states (dashed green curves). Mobility edges at small $|\lambda|$ and at λ in the vicinity of ± 1, the latter barely detectable on the scale of the figure, imply that both very fast and very slow modes correspond to localized states.

The relaxation time spectra of the system studied in Fig. 6 are very broad, our results covering more than five orders of magnitude. For both values of the inverse temperature β, the large τ behaviour of the relaxation time distributions is compatible with a power-law behaviour, $\rho_\tau(\tau) \sim \tau^{-\gamma}$ with $\gamma \simeq 2.23$ at $\beta = 2$, and $\gamma \simeq 1.60$ at $\beta = 5$. A comparison of results for the $\beta = 2$ and the $\beta = 5$ case shows that the spectral density gives more weight to eigenvalues near $\lambda = \pm 1$ as β is increased, entailing that the relaxation time distribution gives more weight to slow modes. In particular, the asymptotic decay of the relaxation-time distribution at large τ, as quantified by the exponent γ, is significantly slower for $\beta = 5$ than it is for $\beta = 2$. Another significant effect of raising the inverse temperature (decreasing the temperature) at which glassy relaxation is studied is to extend the region of localized fast modes to larger τ. Both aspects would clearly deserve a more quantitative and systematic investigation.

It should be noted that resolving both the small and the large τ asymptotics requires analysing spectra at extremely fine resolution, both very close to $\lambda = 0$, and $\lambda = \pm 1$. We do not wish to hide the fact that this is numerically *very* challenging, in particular as the analysis of relaxation time spectra corresponding to localized modes requires keeping small non-zero values for the regularizing parameter ε used in the theory, which induces a smoothing of spectra over scales of the order of ε, and thus tends to deform results in the vicinity of δ-peaks of sizeable weight in the spectrum. In order to keep the effect of such deformation down, we choose a value of $\varepsilon = 10^{-6}$ to properly resolve, in particular, the small τ region of relaxation-time spectra, which, in turn, requires very long measuring runs 'in equilibrium of the population dynamics' to achieve good accuracy. Here is clearly the point where the need for good asymptotic analytic control of eigenvalue spectra is very urgently felt.

6. Summary and discussion

In summary, we have computed spectra of random stochastic matrices which are constructed in terms of random graphs. Our methods used to compute spectra require that the Markov matrices under investigation satisfy a detailed balance condition, or in other words that the Markov chains described by them are time reversible. We expect, however, that this restriction can be overcome by suitably adapting the methods of [46], and we intend to look at this problem in a future publication. The graph ensemble within reach of the present methods is the so-called configuration model, defining an ensemble of graphs that is maximally random, subject only to a given degree distribution. As it stands, we also need to assume that the

mean degree remains finite in the thermodynamic limit. It is clear, however that systems defined on Erdős–Renyi graphs with diverging mean degree are within easy reach of our methods.

Given the ubiquity of systems that can be described in terms of Markov processes defined on complex random graphs, and given the flexibility of our approach, we believe our method and results to hold considerable potential for a broad range of applications.

Using the relation between eigenvalues of stochastic matrices and relaxation-times of Markov processes described by these matrices, we can translate eigenvalue spectra into relaxation time spectra. An example for a generalized trap-model with Kramers transition rates between a network of long-lived states is analyzed in Sec. 5.

Of particular interest is the appearance of localized states in systems of the type described in the present paper. Referring to Eq. (2), two aspects deserve particular mention in this context: *(i)* Eigenvectors $\boldsymbol{v}_\alpha$ corresponding to localized modes are typically supported on a subset of the vertices of a graph that constitutes a vanishingly small fraction of the entire system in the thermodynamic limit; in this sense, these modes only contribute to local probability flows. *(ii)* For localized initial conditions $\boldsymbol{p}(0)$, the projections $(\boldsymbol{w}_\alpha, \boldsymbol{p}(0))$ of initial conditions on (left) eigenvectors corresponding to localized modes will with high probability be vanishingly small in the thermodynamic limit, entailing that the vast majority of localized modes will not contribute to the relaxation dynamics under these circumstances.

Localization effects are traditionally discussed and understood in terms of quantum interference effects [47]. Here we find that localization effects must *generally* be reckoned within the context of classical stochastic dynamics, if the underlying systems exhibit a sufficient degree of heterogeneity, an issue we have not seen much discussed in the literature. Notable recent exceptions include a study of localization effects in so-called maximum-entropy random walks in [48], and a recent observation of localization in a special variant of the periodically kicked rotor [49] which is, in fact, a deterministic classical system.

In the present paper, we have restricted our analysis to 'homogeneously' defined graphs. However, as in the case of adjacency matrices and weighted graph Laplacians, our approach is easily generalized to systems exhibiting modular or small-world properties [50].

Concerning the description of stochastic dynamics, we have here looked at Markov matrices appropriate for the analysis of systems with *discrete-time* dynamics. In the case of *continuous-time* dynamics, one would instead have to look at weighted graph Laplacians as the appropriate infinitesimal generators of dynamics. The spectral theory of these objects was developed in earlier papers [31, 50] for transition matrices which are symmetric to

begin with. Transition matrices which are not symmetric, but satisfy a detailed balance condition would be in reach by combining the symmetrization technique used in the present paper with the methods developed in [31]. A further extension of the current methodology is required, if transition matrix elements depend on *site-randomness* rather than being independently chosen as properties of *links*, the Barrat–Mézard version of the trap model of glassy dynamics [12] with Glauber transition rates being a notable example. At the cost of moderate further complications, such systems can, however, be handled, and we shall report results in a future publication.

Appendix

Replica analysis

In this appendix, we provide a brief account of the replica analysis of the spectral problem for random Markov matrices defined in terms of random graphs; we only document the preparatory stage of the calculation for the special case of unbiased random walks, but provide and account of the full calculation for the case of more general Markov matrices.

Replica analysis — unbiased random walk

Referring to the structure (11) of the symmetrized version $\mathcal{W}$ for of the transition matrix for the unbiased random walk problem, we introduce a decomposition of the system into the set of connected sites $\mathcal{N} = \{i; k_i \neq 0\}$, and its complement $\bar{\mathcal{N}}$, the set of isolated sites. In terms of this decomposition, the partition function (15) allows the decomposition

$$Z_W = Z_{\bar{\mathcal{N}}} \times Z_{\mathcal{N}}\,, \tag{48}$$

with the partition function corresponding to the isolated sites simply given by

$$Z_{\bar{\mathcal{N}}} = (\lambda_\varepsilon - 1)^{-|\bar{\mathcal{N}}|/2}\ . \tag{49}$$

For the partition function corresponding to connected sites, we have

$$Z_{\mathcal{N}} = \int \prod_{i\in\mathcal{N}} \frac{du_i}{\sqrt{2\pi/i}}\ \exp\left\{-\frac{i}{2}\sum_{i,j\in\mathcal{N}}\left(\lambda_\varepsilon\delta_{ij} - \frac{c_{ij}}{\sqrt{k_i k_j}}\right)\ u_i u_j\right\}\ . \tag{50}$$

A transformation of variables $u_i \leftarrow \frac{u_i}{\sqrt{k_i}}$ in the above integral transforms (50) into

$$Z_{\mathcal{N}} = \left(\prod_{i\in\mathcal{N}} k_i\right)^{1/2} \int \prod_{i\in\mathcal{N}} \frac{du_i}{\sqrt{2\pi/i}}\ \exp\left\{-\frac{i}{2}\lambda_\varepsilon\sum_{i\in\mathcal{N}} k_i u_i^2 + \frac{i}{2}\sum_{i,j\in\mathcal{N}} c_{ij}u_i u_j\right\}\ . \tag{51}$$

In terms of this decomposition, one finds

$$\rho_N(\lambda) = p(0)\delta(\lambda - 1) + \frac{1}{\pi N} \operatorname{Re} \sum_{i \in \mathcal{N}} k_i \left\langle u_i^2 \right\rangle , \tag{52}$$

where $\langle \ldots \rangle$ denotes an expectation w.r.t. the complex Gaussian weight in terms of which $Z_{\mathcal{N}}$ is defined.

The replica calculation to perform the average of $\ln Z_{\mathcal{N}}$ can be done using straightforward modifications of those presented for sparse matrices described in detail in [31, 50]. The only subtlety here is that probabilities of coordinations need initially be replaced by conditional probabilities, *given* the coordination is non-zero. We will not reproduce the details here; the interested reader could easily reconstruct them following the outline of the calculation of the more general case documented below.

Here just quote the result. Following [31, 50], one obtains a pair of sef-consistency equations for the saddle point evaluation of the average $\langle Z_{\mathcal{N}}^n \rangle$ of the replicated partition function in a replica symmetric formulation of the problem. These are:

$$\begin{aligned} \hat{\pi}(\hat{\omega}) &= \int d\pi(\omega)\, \delta\left(\hat{\omega} - \hat{\Omega}\right) , \\ \pi(\omega) &= \sum_{k \geq 1} p(k) \frac{k}{c} \int \prod_{\nu=1}^{k-1} d\hat{\pi}\left(\hat{\omega}_\nu\right)\ \delta\left(\omega - \Omega_{k-1}\right) \end{aligned}$$

with $\operatorname{Re}\{\omega, \hat{\omega}\} \geq 0$, and

$$\hat{\Omega} = \hat{\Omega}(\omega) = \frac{1}{\omega} \qquad \text{and} \qquad \Omega_{k-1} = \Omega\left(\{\hat{\omega}_\nu\}_{\nu=1}^{k-1}\right) = i\lambda_\varepsilon k + \sum_{\ell=1}^{k-1} \hat{\omega}_\nu \,. \tag{53}$$

The equations for $\hat{\pi}(\hat{\omega})$ and $\pi(\omega)$ can be combined by inserting the former into the latter, giving

$$\pi(\omega) = \sum_{k \geq 1} p(k) \frac{k}{c} \int \prod_{\nu=1}^{k-1} d\pi(\omega_\nu)\ \delta\left(\omega - \Omega_{k-1}\right) \tag{54}$$

with now

$$\Omega_{k-1} = \Omega\left(\{\omega_\nu\}_{\nu=1}^{k-1}\right) = i\lambda_\varepsilon k + \sum_{\nu=1}^{k-1} \frac{1}{\omega_\nu} \,. \tag{55}$$

In terms of the solution of (28), one obtains the spectral density of W for a random graph with degree distribution $p(k)$ as

$$\rho(\lambda) = p(0)\delta(\lambda - 1) + \frac{1}{\pi}\,\mathrm{Re}\sum_{k\geq 1} p(k) \int \prod_{\nu=1}^{k} d\pi(\omega_\ell)\; \frac{k}{i\lambda_\varepsilon k + \sum_{\nu=1}^{k} \frac{1}{\omega_\nu}}\,, \quad (56)$$

which agrees with the result (30), obtained using a cavity approach.

Replica analysis — general stochastic matrices

As for the transition matrices describing unbiased random walks, we use the natural partition of the system into isolated and connected sites, and introduce a transformation of integration variables $u_i \leftarrow \frac{u_i}{\sqrt{\Gamma_i}}$ on the connected sites to express the analogue of (51) for this case as

$$Z_{\mathcal{N}} = \left(\prod_{i\in\mathcal{N}} \Gamma_i\right)^{1/2} \int \prod_{i\in\mathcal{N}} \frac{du_i}{\sqrt{2\pi/i}}\; \exp\left\{-\frac{i}{2}\lambda_\varepsilon \sum_{i\in\mathcal{N}} \Gamma_i u_i^2 + \frac{i}{2}\sum_{i,j\in\mathcal{N}} c_{ij}K_{ij}\; u_i u_j\right\}. \quad (57)$$

Averaging over the disorder is, in the present case, complicated by the fact that the site-disorder in the $\{\Gamma_i\}$ is correlated with the bond-disorder beyond the constraint that the connectivity matrix is compatible with a given degree sequence, as in the present case the $\Gamma_j = \sum_i c_{ij}K_{ij}$ also depend on the weights connected to a given site. Using this definition of the $\{\Gamma_i\}$ and symmetry of the weights, we can transform (57) into

$$\begin{aligned} Z_{\mathcal{N}} \;=\; & \left(\prod_{i\in\mathcal{N}} \Gamma_i\right)^{1/2} \int \prod_{i\in\mathcal{N}} \frac{du_i}{\sqrt{2\pi/i}} \\ & \times \exp\left\{-\frac{i}{4}\lambda_\varepsilon \sum_{i,j\in\mathcal{N}} c_{ij}K_{ij}\left(u_i^2 + u_j^2\right) + \frac{i}{2}\sum_{i,j\in\mathcal{N}} c_{ij}K_{ij}\; u_i u_j\right\}. \quad (58) \end{aligned}$$

This form is now ready to perform an average over the connectivity matrices and weights defining the Markov matrix ensemble in question. Concerning details, one might either perform the average using a full micro-canonical graph ensemble (as documented in detail for matrices with general modular structure in [50]). There are two possible short-cuts which can simplify the calculation. One can do the calculation for an Erdős–Renyi ensemble of weighted graphs and use the fact that — *formally* — the analysis carries over to more general graph ensembles within the configuration model class,

as was done in [31]. Alternatively, one can perform an average over a *canonical* graph ensemble, and recover micro-canonical results at the end of the calculation, which is the approach we shall take here.

We can omit the prefactor $(\prod_{i\in\mathcal{N}} \Gamma_i)^{1/2}$ from (58), the effects of which are irrelevant when evaluating the spectral density. The canonical distribution of connectivity matrix elements compatible with a degree sequence (k_i) of mean degree c is

$$p(c_{ij}) = \left(1 - \frac{k_i k_j}{cN}\right)\, \delta_{c_{ij},0} + \frac{k_i k_j}{cN}\, \delta_{c_{ij},1}\,, \qquad i<j\,, \tag{59}$$

with $c_{ij} = c_{ji}$. Note that when evaluating $\langle Z_{\mathcal{N}}^n\rangle$, we are looking at a conditional averages, *given* that coordinations are non-zero, so $\tilde{c} = c/(1-p(0))$ is the average coordination on $\mathcal{N}$; this entails that $cN = \tilde{c}|\mathcal{N}|$. The average of the replicated partition function is thus obtained as

$$\langle Z_{\mathcal{N}}^n\rangle \propto \int \prod_{i\in\mathcal{N},a} \frac{du_{ia}}{\sqrt{2\pi/i}} \exp\left\{\frac{\tilde{c}}{2|\mathcal{N}|}\sum_{i,j\in\mathcal{N}} \frac{k_i}{\tilde{c}}\frac{k_j}{\tilde{c}}\right.$$
$$\left.\times\left(\left\langle \exp\left\{iK\sum_a\left[u_{ia}u_{ja} - \frac{i}{2}\lambda_\varepsilon\left(u_{ia}^2+u_{ja}^2\right)\right]\right\}\right\rangle_K - 1\right)\right\}. \tag{60}$$

We now rewrite (60) as a functional integral, using the replica density

$$\rho(\boldsymbol{u}) = \frac{1}{|\mathcal{N}|}\sum_{i\in\mathcal{N}}\frac{k_i}{\tilde{c}}\delta(\boldsymbol{u}-\boldsymbol{u}_i) = \frac{1}{N}\sum_{i\in\mathcal{N}}\frac{k_i}{c}\delta(\boldsymbol{u}-\boldsymbol{u}_i) \tag{61}$$

and its conjugate arising from a Fourier representation of the defining δ-functional as order parameters, giving

$$\langle Z_{\mathcal{N}}^n\rangle \propto \int \mathcal{D}\{\rho,\hat{\rho}\}\exp\{N[G_b+G_m+G_s]\}\,, \tag{62}$$

with

$$G_b = \frac{c}{2}\int d\rho(\boldsymbol{u})d\rho(\boldsymbol{v})$$
$$\times\left(\left\langle\exp\left\{iK\sum_a\left[u_av_a - \tfrac{1}{2}\lambda_\varepsilon\left(u_a^2+v_a^2\right)\right]\right\}\right\rangle_K - 1\right), \tag{63}$$

$$G_m = -\int d\boldsymbol{u}\; i\hat{\rho}(\boldsymbol{u})\rho(\boldsymbol{u})\,, \tag{64}$$

$$G_s = \sum_{k\geq 1} p(k)\ln\int\prod_a\frac{du_a}{\sqrt{2\pi/i}}\exp\left\{i\frac{k}{c}\hat{\rho}(\boldsymbol{u})\right\}. \tag{65}$$

Replica symmetry

Following previous micro-canonical calculations [31, 50], we now use a replica-symmetric ansatz of the form

$$\rho(\boldsymbol{u}) \;=\; \int d\pi(\omega) \prod_a \frac{e^{-\frac{\omega}{2}u_a^2}}{Z(\omega)}\,, \tag{66}$$

$$i\hat{\rho}(\boldsymbol{u}) \;=\; \hat{c}\int d\hat{\pi}(\hat{\omega}) \prod_a \frac{e^{-\frac{\hat{\omega}}{2}u_a^2}}{Z(\hat{\omega})} \tag{67}$$

with

$$Z(\omega) = \sqrt{2\pi/\omega} \tag{68}$$

for the replica-density $\rho(\boldsymbol{u})$ and its conjugate $i\hat{\rho}(\boldsymbol{u})$. Here, π and $\hat{\pi}$ are taken to be normalized probability density functions. For $\hat{\pi}$ to be normalized, the parameter $\hat{c}$ must then be properly chosen. This gives

$$G_b[\pi] \;\simeq\; n\frac{c}{2}\int d\pi(\omega)d\pi(\omega')\;\left\langle \ln\left[\frac{Z_2\left(\omega,\omega',K,\lambda_\varepsilon\right)}{Z(\omega)Z(\omega')}\right]\right\rangle_K\,, \tag{69}$$

$$G_m[\pi,\hat{\pi}] \;\simeq\; -\hat{c} - n\hat{c}\int d\pi(\omega)d\hat{\pi}(\hat{\omega})\;\ln\left[\frac{Z\left(\omega+\hat{\omega}\right)}{Z(\omega)Z(\hat{\omega})}\right]\,, \tag{70}$$

$$\begin{aligned} G_s[\hat{\pi}] \;\simeq\; \hat{c} + n\sum_{k\geq 1}p(k)\sum_{\ell=0}^{\infty}p_\kappa(\ell)\int\prod_{\nu=1}^{\ell}d\hat{\pi}(\hat{\omega}_\nu) \\ \times\ln\left[\frac{Z\left(\sum_{\nu=1}^{\ell}\hat{\omega}_\nu\right)}{\sqrt{2\pi/i}\prod_{\nu=1}^{\ell}Z(\hat{\omega}_\nu)}\right] \end{aligned} \tag{71}$$

as the leading small-n contributions to G_b, G_m and G_s, now expressed as functionals of π and $\hat{\pi}$. Here, $p_\kappa(\ell) = \frac{\kappa^\ell}{\ell!}e^{-\kappa}$ is a Poisson distribution with mean $\kappa \equiv \hat{c}\frac{k}{c}$, and we have defined

$$Z_2\left(\omega,\omega',K,\lambda_\varepsilon\right) = \int dudv\,\exp\left\{iKuv - \tfrac{1}{2}\left(\omega+i\lambda_\varepsilon K\right)u^2 - \tfrac{1}{2}\left(\omega'+i\lambda_\varepsilon K\right)v^2\right\}\,. \tag{72}$$

Note that by doing the v integral in Z_2, one has

$$Z_2(\omega,\omega',K,\lambda_\varepsilon) = Z(\omega'+i\lambda_\varepsilon K)\,Z\left(\omega+i\lambda_\varepsilon K+\frac{K^2}{\omega'+i\lambda_\varepsilon K}\right)\,. \tag{73}$$

Fixed point equations follow from stationarity requirement of the integral (62) w.r.t. variations of the normalized π and $\hat{\pi}$, giving $\hat{c} = c$, hence $\kappa = k$,

and

$$\hat{\pi}(\hat{\omega}) \;=\; \int d\pi(\omega)\;\left\langle \delta\left(\hat{\omega}-\hat{\Omega}(\omega,K,\lambda_\varepsilon)\right)\right\rangle_K\,, \tag{74}$$

$$\pi(\omega) \;=\; \sum_{k\geq 1} p(k)\frac{k}{c}\sum_{\ell=1}^{\infty} p_k(\ell)\frac{\ell}{k}\int\prod_{\nu=1}^{\ell-1} d\hat{\pi}(\hat{\omega}_\nu)\;\delta\left(\omega-\Omega_{\ell-1}\right) \tag{75}$$

with

$$\hat{\Omega}\left(\omega,K,\lambda_\varepsilon\right) \;=\; i\lambda_\varepsilon K+\frac{K^2}{\omega+i\lambda_\varepsilon K}\,, \tag{76}$$

$$\Omega_{\ell-1} \;=\; \sum_{\nu=1}^{\ell-1}\hat{\omega}_\nu\,. \tag{77}$$

For details of the reasoning, we refer to [31, 50]. As before, the two fixed point equations can be combined by inserting the first into the second, giving

$$\pi(\omega)=\sum_{k\geq 1} p(k)\frac{k}{c}\sum_{\ell=1}^{\infty} p_k(\ell)\frac{\ell}{k}\int\prod_{\nu=1}^{\ell-1} d\pi(\omega_\nu)\left\langle\delta\left(\omega-\Omega_{\ell-1}\right)\right\rangle_{\{K_\nu\}}\,, \tag{78}$$

with now

$$\Omega_{\ell-1}=\sum_{\nu=1}^{\ell-1}\left[i\lambda_\varepsilon K_\nu+\frac{K_\nu^2}{\omega_\nu+i\lambda_\varepsilon K_\nu}\right]\,. \tag{79}$$

Results for micro-canonical graph ensembles are recovered by replacing the Poisson distribution $p_k(\ell)$ appearing in the above self-consistency equations by a sharp distribution with all weight concentrated at $\ell=k$, *i.e.* by substituting $p_k(\ell)\to\delta_{\ell k}$. The resulting fixed point equation then agrees with (35), (36), as obtained earlier using a cavity analysis.

REFERENCES

[1] M.E.J. Newman, S.H. Strogatz, D.J. Watts, *Phys. Rev. E* **64**, 026118 (2001).

[2] R. Albert, A.-L. Barabási, *Rev. Mod. Phys.* **74**, 47 (2002).

[3] M.E.J. Newman, *SIAM Rev.* **45**, 167 (2003).

[4] S.N. Dorogovtsev, A.V. Goltsev, J.F.F. Mendes, *Rev. Mod. Phys.* **80**, 1275 (2008).

[5] A. Barrat, M. Barthelemy, A. Vespignani, *Dynamical Processes on Complex Networks*, Cambridge Univ. Press, Cambridge 2008.

[6] F. Spitzer, *Principles of Random Walk*, Springer, 1964.

[7] A.J. Bray, G.J. Rodgers, *Phys. Rev. B* **38**, 11461 (1988).

[8] Y. Moreno, R. Pastor-Satorras, A. Vespignani, *Eur. J. Phys. B* **26**, 521 (2002).

[9] M.E.J. Newman, *Phys. Rev. E* **66**, 016128 (2002).

[10] T. Spyropoulos, K. Psounis, C.S. Raghavendra, *IEEE-ACM T. Network. (TON)* **16**, 63 (2008).

[11] J.-P. Bouchaud, *J. Phys. I* **2**, 1705 (1992).

[12] A. Barrat, M. Mézard, *J. Phys. I* **5**, 941 (1995).

[13] P. Moretti, A. Baronchelli, A. Barrat, R. Pastor-Satorras, *J. Stat. Mech.* **2011**, P03032 (2011).

[14] F. Noé, S. Fischer, *Curr. Opin. Struc. Biol.* **18**, 154 (2008).

[15] D.L. Stein, C.M. Newman, *Nature vs. Nurture in Complex and Not-So-Complex Systems* in: A. Sanayei, I. Zelinka, O.E. Roessler (Eds.), ISCS 2013: Interdisciplinary Symposium on Complex Systems, pp. 57–63, Springer, Heidelberg 2014 [arXiv:1405.7715 [cond-mat.stat-mech]].

[16] S. Brin, L. Page, *Comput. Netw.* **30**, 107 (1998).

[17] L.A. Adamic, R.M. Lukose, A.R. Puniyani, B.A. Huberman, *Phys. Rev. E* **64**, 046135 (2001).

[18] L. Lovász, *Random Walks on Graphs: A Survey*, in: *Combinatorics, Paul Erdős is Eighty*, Vol. 2, Janos Bolyai Mathematical Society, 1993, pp. 1–46.

[19] J.D. Noh, H. Rieger, *Phys. Rev. Lett.* **92**, 118701 (2004).

[20] M. Bonaventura, V. Nicosia, V. Latora, *Phys. Rev. E* **89**, 012803 (2014).

[21] H. Zhou, *Phys. Rev. E* **67**, 041908 (2003).

[22] D. Cvetković, M. Doob, H. Sachs, *Spectra of Graphs — Theory and Applications*, 3rd Edition, J.A. Barth, Heidelberg 1995.

[23] I. Farkas, I. Derény, A.L. Barabási, T. Vicsek, *Phys. Rev. E* **64**, 026704 (2001).

[24] S.N. Dorogovtsev, A.V. Goltsev, J.F.F. Mendes, A.N. Samukhin, *Phys. Rev. E* **68**, 046109 (2003).

[25] P.N. McGraw, M.Menzinger, *Phys. Rev. E* **77**, 031102 (2008).

[26] A.N. Samukhin, S.N. Dorogovtsev, J.F.F. Mendes, *Phys. Rev. E* **77**, 036115 (2008).

[27] G.J. Rodgers, A.J. Bray, *Phys. Rev. B* **37**, 3557 (1988).

[28] G. Biroli, R. Monasson, *J. Phys. A* **32**, L255 (1999).

[29] G. Semerjian, L.F. Cugliandolo, *J. Phys. A* **35**, 4837 (2002).

[30] D.S. Dean, *J. Phys. A* **35**, L153 (2002).

[31] R. Kühn, *J. Phys. A* **41**, 295002 (2008).

[32] T. Rogers, I. Pérez Castillo, R. Kühn, K. Takeda, *Phys. Rev. E* **78**, 031116 (2008).

[33] C. Bordenave, P. Caputo, D. Chafaï, *ALEA* **7**, 41 (2010) [arXiv:0811.1097 [math.PR]].

[34] C. Bordenave, P. Caputo, D. Chafaï, *Probab. Theory Rel.* **152**, 751 (2012).
[35] C. Bordenave, P. Caputo, D. Chafaï, *Commun. Pur. Appl. Math.* **67**, 621 (2014).
[36] C. Grabow, S. Grosskinsky, M. Timme, *Phys. Rev. Lett.* **108**, 218701 (2012).
[37] T.P. Peixoto, *Phys. Rev. Lett.* **111**, 098701 (2013).
[38] Z. Zhang, X. Guo, Y. Lin, *Phys. Rev. E* **90**, 022816 (2014).
[39] R. Kühn, *Europhys. Lett.* **109**, 60003 (2015).
[40] F.R. Gantmacher, *Applications of the Theory of Matrices*, Interscience, New York 1959.
[41] G. Tanner, *J. Phys. A* **34**, 8485 (2001).
[42] K. Zyczkowski, M. Kus, W. Slomczynski, H.J. Sommers, *J. Phys. A* **36**, 3425 (2003).
[43] V. Cappellini, H.J. Sommers, W. Bruzda, K. Zyczkowski, *J. Phys. A* **42**, 365209 (2009).
[44] S.F. Edwards, R.C. Jones, *J. Phys. A* **9**, 1595 (1976).
[45] B.D. McKay, *Linear Algebra Appl.* **40**, 203 (1981).
[46] T. Rogers, I. Pérez Castillo, *Phys. Rev. E* **79**, 012101 (2009).
[47] P.W. Anderson, *Phys. Rev.* **25**, 1492 (1958).
[48] Z. Burda, J. Duda, J.M. Luck, B. Waclaw, *Phys. Rev. Lett.* **102**, 160602 (2009).
[49] I. Guarneri, G. Casati, V. Karle, *Phys. Rev. Lett.* **113**, 174101 (2014).
[50] R. Kühn, J. van Mourik, *J. Phys. A* **44**, 165205 (2011).